Progress In Electromagnetics Research B, Vol. 36, 373–398, 2012

BROADBAND TRANSMISSION CHARACTERISTICS OF OVERHEAD HIGH-VOLTAGE POWER LINE COMMUNICATION CHANNELS

A. G. Lazaropoulos*

Zografou Campus, School of Electrical and Computer Engineering, National Technical University of Athens, 9, Iroon Polytechneiou Street, Athens, GR 15780, Greece

Abstract—This paper considers broadband signal transmission via high-voltage/broadband over power lines (HV/BPL) channels associated with overhead power transmission. To determine the end-to-end channel characteristics of various overhead HV/BPL multiconductor transmission line (MTL) configurations, the chain scattering matrix or T-Matrix (TM) method is adopted. The overhead HV/BPL transmission channel is investigated with regard to its spectral behavior, its end-to-end signal attenuation, and phase response. It is found that the above features depend critically on the frequency, the coupling scheme applied, the physical properties of the cables used, the MTL configuration, and the type of branches existing along the end-to-end BPL signal propagation. Unlike the older models that underestimate the broadband transmission potential of overhead HV lines significantly, the results demonstrate that the overhead HV grid is a potentially excellent communications medium, offering low loss characteristics over a 100 km repeater span well beyond 100 MHz and guarantees the imminent coexistence of low-voltage (LV), medium-voltage (MV), and HV BPL systems towards a unified transmission/distribution smart grid (SG) power grid.

1. INTRODUCTION

Due to ubiquitous nature of the low-voltage (LV), medium-voltage (MV), and high-voltage (HV) power grids, the structure of these grids is the key to developing an advanced IP-based power system, offering a plethora of potential smart grid (SG) applications, such as

Received 14 September 2011, Accepted 8 November 2011, Scheduled 26 November 2011
* Corresponding author: Athanasios G. Lazaropoulos (AGLazaropoulos@gmail.com).

ubiquitous grid surveillance at small cost, continuous monitoring, real time adjustment of sensitive loads, and optimal response to power demand during critical circumstances [1–3]. Moreover, the need for delivering broadband last mile access in remote and/or underdeveloped areas provides a strong motivation for the deployment of broadband over power lines (BPL) networks through the entire grid [4–11].

The first power line communications (PLC) efforts put in place by power utilities over HV lines in the early 1920s with the goal of providing operational telephone services and data communications across large geographical distances [12–15]. Today, although the more significant transformation to upcoming SG technology is expected to take place on the MV and LV distribution power grids, the HV transmission power grids will have to catch the train of upcoming BPL/SG changes [16–20].

Utilities employ either the overhead or the underground HV transmission power grid for new urban, suburban, and rural installations. The choice is made according to different criteria like cost requirements, existing grid topology, and urban plan constraints [20–27].

When considered as a transmission medium for communications signals, the overhead and underground power grids are subjected to attenuation, multipath due to various reflections, noise, and electromagnetic interference (EMI) [28–36]. Each of the aforementioned adverse factors affects the overall performance and the design of BPL systems [37–40].

Due to the evolution of broadband communications and SG applications, the development of accurate models to describe signal transmission at high frequencies along the HV transmission power lines is essential. As usually done in LV/BPL and MV/BPL transmission, a hybrid model is employed to examine the behavior of BPL transmission channels installed on BPL multiconductor transmission line (MTL) structures [5, 28–30, 41–46]. This hybrid model follows: (i) a bottom-up approach consisting of an appropriate combination of similarity transformations and MTL theory to determine the propagation constant and the characteristic impedance of the modes supported [40–52]; and (ii) a top-down approach based either on multipath-model presented in [22, 37, 53, 54] or on cascaded matrices of two-port network modules to determine the end-to-end attenuation and phase response of BPL channel connections [22, 30, 31, 37, 41, 43, 45, 49, 52, 55, 56]. In this paper, the chain scattering matrix or T-matrix (TM) method, which is outlined in [30, 41, 52, 56], is applied to evaluate the HV/BPL channel characteristics.

The hybrid model approach, based on *a priori* computations, takes into account accurately determined parameters such as the MTL configuration and grid topology. This approach is flexible and accurate determining, consequently, any changes of the transfer characteristics related to relevant factors of the HV/BPL system configuration [42, 45, 49, 55, 57]. The influence of factors, such as the physical properties of the cables used, the MTL configuration, the coupling scheme applied, the end-to-end distance, and the number and the electrical length encountered along the end-to-end HV/BPL signal propagation are investigated based on numerical results concerning simulated overhead HV/BPL topologies.

The rest of this paper is organized as follows: In Section 2, the modal behavior of BPL propagation is discussed along with the necessary assumptions concerning overhead HV/BPL transmission. Section 3 deals with signal transmission via power lines by the TM method which is applied for the evaluation of the end-to-end modal transfer functions. In Section 4, numerical results are provided, aiming at marking out how the various features of the overhead HV transmission power grids influence BPL transmission. Section 5 concludes the paper.

2. THE PHYSICAL BPL LAYER

The overhead HV power grid differs considerably from transmission via twisted-pair, coaxial, or fiber-optic cables due to the significant differences of the network structure and the physical properties of the power cables used [7, 21, 22, 29, 31, 34, 41, 42, 55].

A typical case of 150 kV single-circuit overhead HV transmission line is depicted in Fig. 1. Three parallel phase conductors spaced by Δ_p in the range from 6.60 m to 8.95 m are suspended at heights h_p ranging from 19 m to 19.95 m above lossy ground — conductors 1, 2, and 3 —. Moreover, two parallel neutral conductors spaced by Δ_n in the range from 9.30 m to 12.10 m hang at heights h_n ranging from 23.75 m to 24.7 m — conductors 4 and 5 —. This three-phase five-conductor overhead HV distribution line configuration is considered in the present work consisting of ACSR GROSBEK $3 \times 374.77\,\mathrm{mm}^2 + 2 \times 322.26\,\mathrm{mm}^2$ conductors [25–27, 58–61].

The ground is considered as the reference conductor. The conductivity of the ground is assumed $\sigma_g = 5\,\mathrm{mS/m}$ and its relative permittivity $\varepsilon_{rg} = 13$, which is a realistic scenario [7, 28, 41, 42, 55]. The impact of imperfect ground on signal propagation over overhead power lines was analyzed in [28, 41, 42, 55, 57, 62–64]. This formulation has the advantage that, contrary to other available models for overhead power lines [65–68], it is suitable for transmission at high frequencies above lossy ground and for broadband applications of overhead LV/BPL, MV/BPL, and HV/BPL systems.

Through a matrix approach, the standard TL analysis can be extended to the MTL case which involves more than two conductors. Compared to a two-conductor line supporting one forward- and one backward-traveling wave, an MTL structure with $n+1$ conductors parallel to the z axis as depicted in Fig. 1 may support n pairs of forward- and backward-traveling waves with corresponding propagation constants. These waves may be described by a coupled set of $2n$ first-order partial differential equations relating the line voltages $V_i(z,t)$, $i=1,\ldots,n$ to the line currents $I_i(z,t)$, $i=1,\ldots,n$. Each pair of forward- and backward-traveling waves is referred to as a mode [29, 41, 47, 48].

In the case of overhead HV distribution lines involving three-phase conductors and two neutral conductors ($n=5$) over lossy plane ground, five modes may be supported, namely [2, 7, 20, 21, 24, 25, 41–44, 47–50, 55, 57–59, 62–64, 69–71]:

- *Common mode* (CM, $i=1$) of overhead HV/BPL transmission which propagates via the five conductors and returns via the ground. γ_{CM} constitutes the CM propagation constant.
- *Differential modes* (DMs) of overhead HV/BPL transmission (DM_{i-1}, $i=2,3,4,5$) which propagate and return via the five

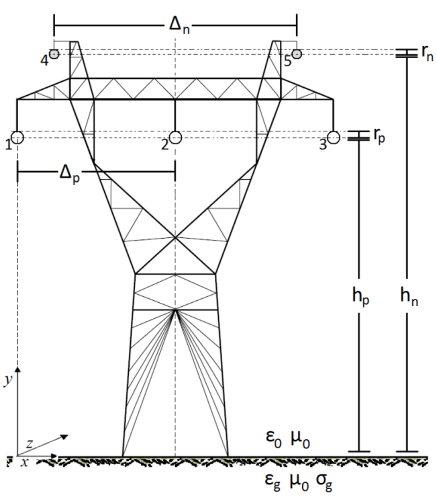

Figure 1. Typical 150 kV single-circuit overhead HV multiconductor structure [25, 58–61].

conductors. γ_{DMi-1}, $i = 2, \ldots, 5$ constitute the propagation constants of DM_{i-1}, $i = 2, \ldots, 5$, respectively.

The attenuation coefficients $\alpha_{CM} = \mathrm{Re}\{\gamma_{CM}\}$ and $\alpha_{DMi-1} = \mathrm{Re}\{\gamma_{DMi-1}\}$, $i = 2, \ldots, 5$ of the CM and the four DMs, respectively, are evaluated using the method presented in [20, 24, 25, 28, 41, 42, 55, 57–59, 62–64, 70, 71] and are plotted versus frequency in Fig. 2(a) for the configuration depicted in Fig. 1. The absolute value of phase delays $\beta_{CM} = \mathrm{Im}\{\gamma_{CM}\}$ and $\beta_{DMi-1} = \mathrm{Im}\{\gamma_{DMi-1}\}$, $i = 2, \ldots, 5$ of the CM and the four DMs, respectively, [20, 24, 25, 28, 41, 42, 55, 57–59, 62–64, 70, 71] are also plotted versus frequency in Fig. 2(b).

As far as the spectral behavior of the modes is concerned, the following characteristics should be noted

(i) As it concerns the overhead HV/BPL transmission channels, in the lower part of the frequency spectrum — up to approximately 20 MHz — the attenuation coefficient of the CM is higher compared to that of the other DMs; hence, practically, only the DMs propagate. The opposite is observed at frequencies above 20 MHz, where the CM and the DMs coexist resulting

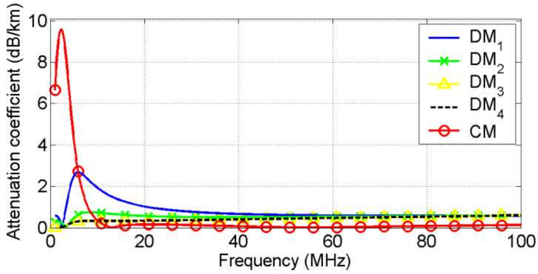

(a)

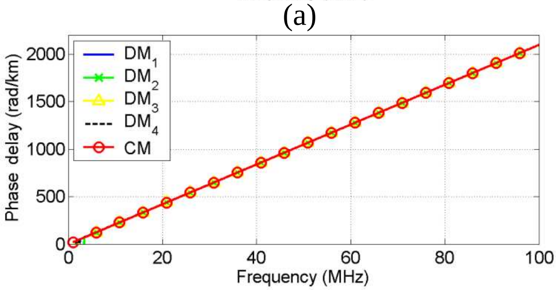

(b)

Figure 2. Frequency spectra of an 150 kV single-circuit overhead HV multiconductor structure (the subchannel frequency spacing is equal to 0.1 MHz). (a) Attenuation coefficients. (b) Phase delays.

to multimode propagation. The shape of CM is explained by considering that at high frequencies the penetration depth into the lossy ground becomes negligible compared to the wavelength; therefore, propagation takes place entirely above the ground as in the lossless case. The peak exhibited by CM is attributed to the resonance occurring inside the ground which, as frequency increases, is initially inductive and, then, capacitive. As to the DMs of overhead HV/BPL transmission, since the relevant influence of the lossy ground is negligible, the DMs attenuation coefficients are primarily affected by the losses and the skin-effect in the conductors. This almost identical spectral behavior of attenuation coefficients has also been observed in overhead LV/BPL and MV/BPL transmission [28, 29, 32, 33, 41, 42, 55, 57, 63, 64, 72–74].

(ii) The phase delays of the CM and the DMs exhibit a linear behavior with respect to frequency and depend on the surrounding media (air) properties. This almost identical spectral behavior of phase delays has also been observed in overhead and underground LV/BPL and MV/BPL transmission [22, 26–29, 32, 33, 42, 43, 46, 49, 50, 55, 57, 72–74].

As it has already been presented in [25, 28, 29, 41, 70], the modal voltages $\mathbf{V}^m(z) = [V_1^m(z) \ \ldots \ V_5^m(z)]^T$ and the modal currents $\mathbf{I}^m(z) = [I_1^m(z) \ \ldots \ I_5^m(z)]^T$ may be related to the respective line quantities $\mathbf{V}(z) = [V_1(z) \ \ldots \ V_5(z)]^T$ and $\mathbf{I}(z) = [I_1(z) \ \ldots \ I_5(z)]^T$ via the similarity transformations [29, 41, 43, 47, 48]

$$\mathbf{V}(z) = \mathbf{T}_V \cdot \mathbf{V}^m(z) \tag{1}$$

$$\mathbf{I}(z) = \mathbf{T}_I \cdot \mathbf{I}^m(z) \tag{2}$$

where $[\cdot]^T$ denotes the transpose of a matrix, $\mathbf{T}_V$ and $\mathbf{T}_I$ are 5×5 matrices depending on the frequency, the physical properties of the cables, and the geometry of the MTL configuration [20, 24, 25, 29, 41, 43, 47, 48, 58, 59, 70, 71]. Through the aforementioned equations, the line voltages and currents are expressed as appropriate superpositions of the respective modal quantities. From (1)

$$\mathbf{V}^m(0) = \mathbf{T}_V^{-1} \cdot \mathbf{V}(0) \tag{3}$$

The above modes excited — each with its own propagation characteristics — may be examined separately across the overall overhead HV transmission network, under the following three assumptions [28, 41–43, 46, 51]:

A1. Cables with identical eigenmodes are used throughout the network. The branches and termination points are perfectly balanced ensuring that there is no mode mixing anywhere in the network.

A2. The branching cables are identical to the transmission cables and the mode propagation constants of all the cable segments are assumed to be the same.

A3. The termination points behave independently of frequency since they are either ideal matches — achieved using adaptive modal impedance matching [75, 76] — or open circuit terminations.

The three assumptions were already made in the analysis of LV/BPL and MV/BPL transmission [28, 30, 41–43, 46, 51]. They are necessary to validate a simple model, so that a more thorough view of the channel attenuation due to cable losses, branches and terminations may be established. Because of the above assumptions, the five modes supported by the overhead HV/BPL configuration are completely separate giving rise to five independent transmission channels which simultaneously carry BPL signals. This complete mode separation along the entire overhead HV/BPL transmission network has also been encountered in overhead LV/BPL and MV/BPL transmission where four and three modes, respectively, exist [28–30, 41, 42, 72].

The TM method — considered in Section 3 — models the spectral relationship between $V_i^m(z)$, $i = 1, \ldots, 5$ and $V_i^m(0)$, $i = 1, \ldots, 5$ proposing operators $H_i^m(z)$, $i = 1, \ldots, 5$ so that

$$\mathbf{V}^m(z) = \mathbf{H}^m\left\{\mathbf{V}^m(0)\right\} \tag{4}$$

where

$$\mathbf{H}^m\left\{\cdot\right\} = \mathrm{diag}\{H_1^m\left\{\cdot\right\} \ldots H_5^m\left\{\cdot\right\}\} \tag{5}$$

is a diagonal matrix operator whose elements $H_i^m(z)$, $i = 1, \ldots, 5$ are the modal transfer functions [28, 29, 41]. Combining (1) and (5), the 5×5 matrix channel transfer function $\mathbf{H}\{\cdot\}$ relating $\mathbf{V}(z)$ with $\mathbf{V}(0)$ through

$$\mathbf{V}(z) = \mathbf{H}\left\{\mathbf{V}(0)\right\} \tag{6}$$

is determined from

$$\mathbf{H}\left\{\cdot\right\} = \mathbf{T}_V \cdot \mathbf{H}^m\{\cdot\} \cdot \mathbf{T}_V^{-1} \tag{7}$$

Based on (5), the 5×5 matrix transfer function $\mathbf{H}\{\cdot\}$ of the overhead HV/BPL transmission network is determined. Similar expressions have been derived in the overhead LV/BPL and MV/BPL cases [28–30, 41, 44, 69].

According to how signals are injected onto overhead HV/BPL transmission lines, two different coupling schemes exist [29, 73, 77]:

- *Wire-to-Wire* (WtW) when the signal is injected between two conductors; say between conductors p and $q \neq p$, $p, q = 1, \ldots, 5$. For the WtW coupling configurations, the relative excitation voltage relationship which is applied to the five conductors at $z = 0$ is given by

$$\mathbf{V}(0) = V^{WtW}(0) \cdot \mathbf{C}^{WtW} \tag{8}$$

where $V^{WtW}(0)$ is the source equivalent Thévenin dipole voltage and $\mathbf{C}^{WtW}$ is the 5×1 WtW coupling column vector with zero elements except in rows p and q where the values are equal to 0.5 and -0.5, respectively. Following the same procedure, the load equivalent Thévenin dipole voltage $V^{WtW}(z)$ is given from

$$V^{WtW}(z) = \left[\mathbf{C}^{WtW}\right]^T \cdot \mathbf{V}(z) \tag{9}$$

Combining (6), (7), (8), and (9), the coupling WtW channel transfer function $H^{WtW}\{\cdot\}$ is determined by

$$H^{WtW}\{\cdot\} = \left[\mathbf{C}^{WtW}\right]^T \cdot \mathbf{T}_V \cdot \mathbf{H}^m\{\cdot\} \cdot \mathbf{T}_V^{-1} \cdot \mathbf{C}^{WtW} \tag{10}$$

WtW coupling between conductors p and q will be detoned as WtW^{p-q}, hereafter.

- *Wire-to-Ground* (WtG) when the signal is injected onto one conductor and returns via the ground; say between conductor s, $s = 1, \ldots, 5$ and the ground. Similar expressions with (10) may be derived in WtG coupling configurations. The coupling WtG channel transfer function $H^{WtG}\{\cdot\}$ is given from

$$H^{WtG}\{\cdot\} = \left[\mathbf{C}^{WtG}\right]^T \cdot \mathbf{T}_V \cdot \mathbf{H}^m\{\cdot\} \cdot \mathbf{T}_V^{-1} \cdot \mathbf{C}^{WtG} \tag{11}$$

where $\mathbf{C}^{WtG}$ is the 5×1 WtG coupling column vector with zero elements except in row s where the value is equal to 1. WtG coupling between conductor s and ground will be detoned as WtG^s, hereafter.

When WtW injection is done, the DMs are mainly excited, whereas the primary excitation of the CM is generated due to the lack of symmetry of the cable configuration; hence, BPL transmission is accomplished mostly via the DMs. This has also observed in WtW injection in overhead MV/BPL transmission and in Phase-to-Phase (PtP) injection in underground MV/BPL transmission [7, 28–30, 41, 42, 55, 62, 72, 77].

When WtG injection is applied, both the CM and DMs are excited. This has also been observed in WtG injection in overhead MV/BPL transmission and in Shield-to-Phase (StP) injection in underground MV/BPL transmission [7, 28–30, 41, 42, 55, 62, 72, 77].

3. EVALUATION OF THE END-TO-END MODAL TRANSFER FUNCTION

In this paper, the TM method will be used to determine the modal transfer function of the independent modal BPL transmission channel in the light of scattering matrix theory [30, 41, 52, 56]. TM method is presented analytically in [30].

To apply the TM method, an end-to-end overhead BPL connection is separated into elementary segments — network modules —, each of them comprising the successive branches encountered — see Fig. 3(a) —. Signal transmission through the various network modules is taken into account based on the respective chain scattering matrices. A typical overhead BPL end-to-end connection comprises branch-type network modules, as depicted in Fig. 3(b), while A and B are assumed matched to the characteristic impedance of the mode considered [22, 37, 42].

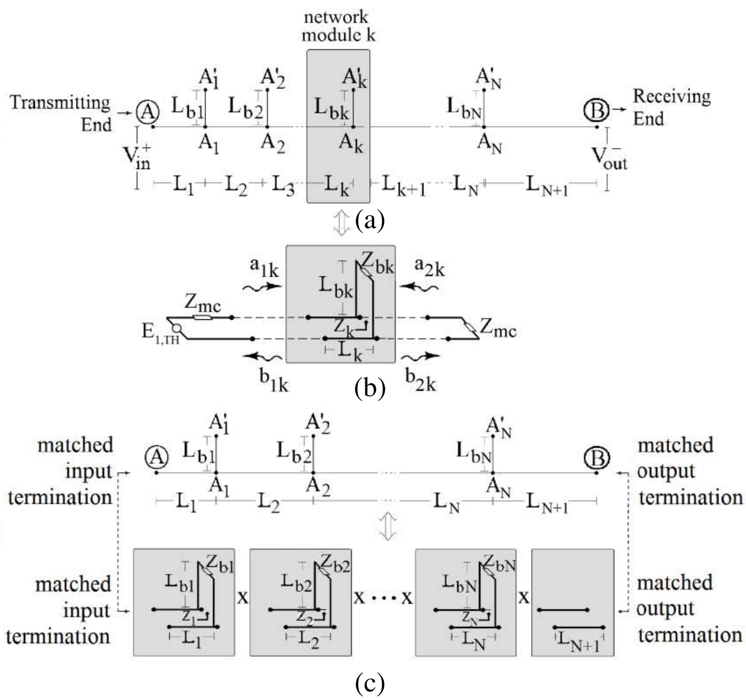

Figure 3. (a) End-to-end BPL connection with N branches. (b) Network module. (c) An indicative BPL topology considered as a cascade of $N+1$ modules corresponding to N branches [28, 30].

To determine the end-to-end modal transfer function one has to evaluate:

1. the scattering matrices $\mathbf{S}_k$, $k = 1, 2, \ldots, N+1$ of the network modules;
2. the respective chain scattering matrices $\mathbf{T}_k$, $k = 1, 2, \ldots, N+1$;
3. the chain scattering matrix $\mathbf{T}_{overall}$ of the end-to-end connection considered as a cascade of $N+1$ network modules, that is, $\mathbf{T}_{overall} = \prod_{k=1}^{N+1} \mathbf{T}_k$; and
4. the respective end-to-end $\mathbf{S}_{overall}$ matrix from

$$\mathbf{S}_{overall} = \begin{bmatrix} \frac{T_{21}}{T_{11}} & T_{22} - \frac{T_{21} \cdot T_{12}}{T_{11}} \\ \frac{1}{T_{11}} & -\frac{T_{12}}{T_{11}} \end{bmatrix} \tag{12}$$

where T_{pq}, $p,q = 1, 2$, are the elements of $\mathbf{T}_{overall}$.

The end-to-end modal transfer function is given by the element S_{21} of the matrix $\mathbf{S}_{overall}$ of (12), that is

$$H_i^m \{\cdot\} = H_i^m(f) = S_{21} = \frac{1}{T_{11}}, \; i = 1, \ldots, 5 \tag{13}$$

4. NUMERICAL RESULTS AND DISCUSSION

The simulations of various types of overhead HV/BPL transmission channels aim at investigating: (a) their broadband transmission characteristics; and (b) how their spectral behavior is affected by the overhead grid topology. As mentioned in Section 2, since the modes supported by the overhead HV/BPL configurations may be examined separately, it is assumed for simplicity that the BPL signal is injected directly into the modes [28–30, 41–45, 47–51, 55]; thus, the complicated modal analysis of [47, 48], briefly described in Section 2, is avoided.

For the numerical computations, the three-phase five-conductor overhead HV transmission line configuration depicted in Fig. 1, has been considered. As previously mentioned, the modes supported by the overhead HV/BPL cable configuration may be examined separately. The following discussion will focus on the transmission characteristics related to: (i) the CM and the DMs of the overhead HV/BPL systems; and (ii) the WtW and the WtG coupling schemes related to overhead HV/BPL systems, as well.

The simple overhead HV/BPL topology of Fig. 3(a), having N branches has been considered. With reference to Fig. 3(c), the transmitting and the receiving ends are assumed matched to the characteristic impedance of the mode considered, whereas the branch terminations Z_{bk}, $k = 1, 2, \ldots, N$ are assumed open circuit [2, 25, 28–30, 41, 42, 58–60, 70].

Today, thousands of HV lines are installed in more than 120 countries for a total length of some millions of km. These lines stretch from approximately 25 km to 190 km from the generator before reaching any population centers. Consequently, average path lengths up to 100 km are encountered in the overhead HV case. Shorter branches in the range of 10 km to 50 km are used in order to connect HV transmission lines either between them or with HV/MV substations [2, 5, 21, 25–27, 58–60, 70, 78, 79].

To compare the equivalent modal with the coupling scheme channels, the following representative overhead HV/BPL topology has been examined — see Fig. 3(c) —:

- The "LOS" transmission along the average end-to-end distance $L = L_1 + \ldots + L_{N+1} = 100$ km when no branches are encountered. This topology corresponds to Line-of-Sight transmission in wireless channels.

In Figs. 4(a) and 4(c), the end-to-end channel attenuation and the phase response, respectively, are plotted versus frequency for the "LOS" transmission case for the propagation of DM_1, DM_2, DM_3, DM_4, and CM. Among the twenty possible WtW and five possible WtG configurations, in Figs. 4(b) and 4(d), the end-to-end coupling channel attenuation and the phase response, respectively, for the "LOS" transmission case for the coupling schemes WtW^{1-2}, WtW^{2-1}, WtW^{1-3}, WtW^{5-2}, WtG^1, and WtG^4 are plotted versus frequency.

The "LOS" transmission channels present low-loss characteristics at frequencies ranging from 1 MHz to 100 MHz over a 100 km repeater span. The fact that overhead HV/BPL lines resemble a low loss transmission system shows as an attractive alternative broadband technology [25, 28–30, 41–43, 49, 55, 60]. Comparing Figs. 4(a), 4(b), 4(c), and 4(d), as it has already been mentioned, WtW coupling schemes are primarily affected by the propagation of DMs, whereas WtG coupling schemes are influenced by CM. Moreover, WtW^{1-2} and WtW^{2-1} present identical spectral behavior validating channel isotropy characterizing BPL point-to-point links [5, 46, 58, 59, 70, 78].

Theoretically, EMI problems are caused by both the CM and the four DMs. Practically, EMI caused by the DM modes is not considered significant because the far field radiation caused by each DM mode is zero. However, the CM current flow may cause significant EMI levels [10, 80–83]. As BPL transmission is primarily accomplished by the DM currents [80], any unintentional transmission on the CM current flow — generated by unbalances of the power line cables which

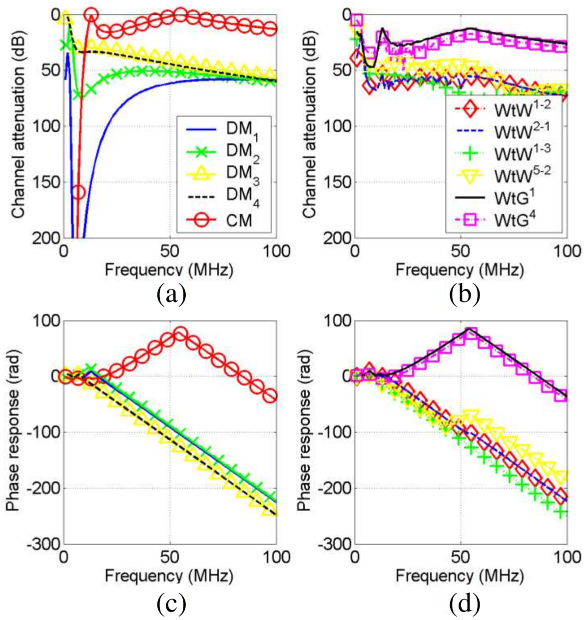

Figure 4. Channel characteristics versus frequency for "LOS" transmission case (the subchannel frequency spacing is equal to 1 MHz). (a), (c) End-to-end attenuation and phase response for modal channels. (b), (d) End-to-end attenuation and phase response for coupling scheme channels.

convert part of the injected/transmitted DM signals into CM signals — should be avoided, since the CM current flow is the main cause of EMI from BPL networks [81]. Nevertheless, as it is observed in Fig. 4(b), the WtG coupling schemes are favorable in comparison with WtW ones due to their lower channel attenuation. Hence, a trade-off between EMI protection and BPL channel attenuation/capacity is outlined.

However, as usually done to simplify the analysis and due to relatively comparable results among modal and coupling scheme channels — as it concerns the end-to-end attenuation and the phase response of the "LOS" transmission case — [13, 17, 28–31, 42, 55, 59, 72, 84], only one mode — say DM_4 — for overhead HV/BPL system will be examined, hereafter. This assumption does not affect the generality of the analysis concerning the transmission characteristics of the examined HV/BPL systems in the range from 1 MHz to 100 MHz, provides a representative picture of the real world overhead HV/BPL network situation, and is adopted for the sake of terseness and simplicity.

With reference to Fig. 3(c), five indicative overhead HV topologies, concerning end-to-end connections of average lengths equal to 100 km, have been examined. These topologies are the "LOS" transmission topology referred to above and [2, 21, 25, 58–60, 70, 78, 79]:

1. A typical urban topology (urban case A) with $N = 3$ branches ($L_1 = 4.6$ km, $L_2 = 48.5$ km, $L_3 = 33.7$ km, $L_4 = 13.2$ km, $L_{b1} = 27.6$ km, $L_{b2} = 17.2$ km, $L_{b3} = 33.1$ km). This topology supplies energy one large residential area and one major city.
2. An aggravated urban topology (urban case B) with $N = 4$ branches ($L_1 = 0.5$ km, $L_2 = 15.8$ km, $L_3 = 13.1$ km, $L_4 = 55.5$ km, $L_5 = 15.1$ km, $L_{b1} = 19$ km, $L_{b2} = 22.7$ km, $L_{b3} = 17.1$ km, $L_{b4} = 18$ km). This topology supplies energy two major cities.
3. A typical suburban topology (suburban case) with $N = 2$ branches ($L_1 = 36.1$ km, $L_2 = 51$ km, $L_3 = 12.9$ km, $L_{b1} = 46.8$ km, $L_{b2} = 13.4$ km). This topology describes three nodes of a ring HV line connection.
4. A typical rural topology (rural case) with only $N = 1$ branch ($L_1 = 15$ km, $L_2 = 85$ km, $L_{b1} = 21.1$ km). This topology carries power to a city located 15 km from the generator.

In Figs. 5(a) and 5(b), the end-to-end channel attenuation and the phase response, respectively, are plotted with respect to frequency for the aforementioned five indicative topologies for the propagation of DM_4. As it has already been investigated in [22, 28, 30, 37, 41, 73, 74, 85, 86], the spectral behavior of the end-to-end channel attenuation depends drastically on the frequency, the physical properties of the cables used, the end-to-end — "LOS" — distance, and the number and the electrical length of the branches encountered along the end-to-end transmission path. However, phase responses present a rather identical linear behavior versus frequency regardless of the overhead HV/BPL topology.

According, mainly, to the picture obtained from their spectral behavior of channel attenuation — see Fig. 5(a) —, the overhead BPL topologies may be classified into three major channel classes (see also [28–30, 40, 84] for other LV/BPL and MV/BPL channels):

- *"LOS" channels*, when no branches are encountered and, consequently, no spectral notches are observed. This case corresponds to the best possible overhead HV/BPL transmission conditions, encountered primarily in rural areas where long-distance transmission occurs.
- *Good channels*, when the number of branches is small and their electrical length is large. Shallow spectral notches are

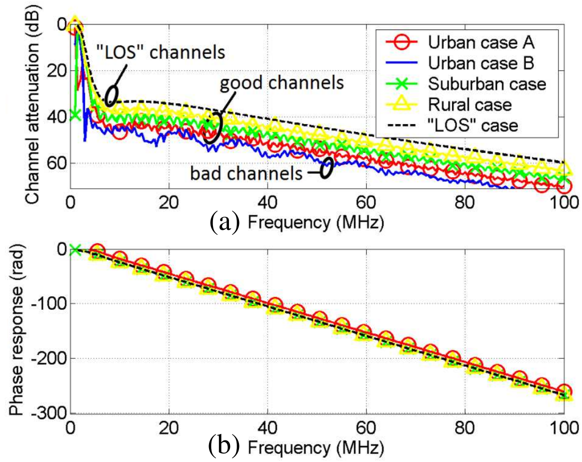

Figure 5. Channel characteristics of DM_4 versus frequency for urban case A, urban case B, suburban case, rural case, and "LOS" transmission case (the subchannel frequency spacing is equal to 0.5 MHz). (a) End-to-end channel attenuation. (b) Phase response.

observed. Overhead HV/BPL transmission primarily near rural and suburban areas belongs to this channel class.

- *Bad channels*, when the number of branches is large and their electrical length is small. Deep spectral notches are observed. Overhead HV/BPL transmission near major cities and large residential areas belongs to this channel class.

The spectral behavior of the above overhead HV/BPL channel classes affects critically the transmission characteristics of overhead BPL channels.

Apart from causing spectral notches, the various branches also cause additional stepwise discontinuities to the channel attenuation at each branch encountered along the end-to-end transmission path. The attenuation discontinuity at each branch is examined in Figs. 6(a) and 6(b), where the channel attenuation of DM_4 is plotted versus the distance from the transmitting end — see Fig. 3(a), point A — for the above five indicative topologies at $f = 25$ MHz and $f = 75$ MHz, respectively. In Figs. 6(c) and 6(d), the respective phase response curves are also plotted in relation with the distance from the transmitting end at $f = 25$ MHz and $f = 75$ MHz, respectively.

Observing Figs. 6(a), 6(b), 6(c), and 6(d), several useful remarks may be drawn.

- Due to reflections and multipath propagation caused by branches, spectral notches are observed in the channel attenuation, which

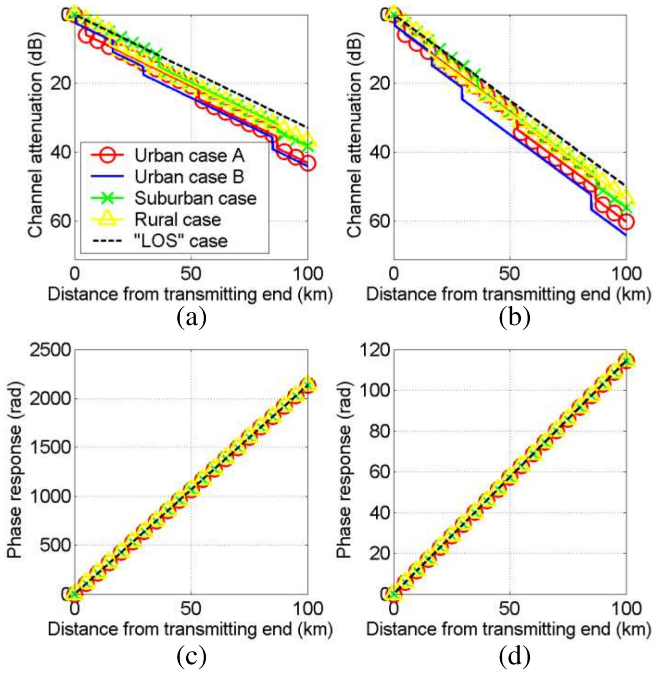

Figure 6. Channel characteristics of DM_4 versus the distance from the transmitting end — see Fig. 3(a), point A — for urban case A, urban case B, suburban case, rural case, and "LOS" transmission case (the distance span is equal to 100 m). (a), (c) Channel attenuation and phase response at $f = 25\,\text{MHz}$. (b), (d) Channel attenuation and phase response at $f = 75\,\text{MHz}$.

are superimposed on the exponential "LOS" attenuation. Unlike channel attenuation, phase response curves present a frequency-selective linear overlapping behavior versus the distance from the transmitting end regardless of the overhead HV/BPL topology considered.

- In most overhead HV/BPL channels, "LOS" distance rather than multipath is identified as the dominant attenuation factor affecting signal transmission. Therefore, in urban and suburban environments denser overhead HV/BPL networks are preferable. The respective shorter end-to-end connections are primarily affected by multipath [5, 25–27, 58–60, 70, 78, 87].
- The attenuation discontinuity at each branch depends on the frequency and on its electrical length. As the branches become

longer, the spectral behavior of the BPL networks tends to converge to the spectral behavior of the respective BPL networks with branch terminations matched to the characteristic impedance of the mode examined; namely, approximately a two-way power divider per each branch [22, 31, 37, 74, 79, 85].

To demonstrate the spectral effect of branch length on the attenuation discontinuity at each branch, in Fig. 7(a), the attenuation discontinuity of DM_4 at the first branch — point A_1, see Fig. 3(a) — is plotted versus frequency for the urban case B, Topology 1 — same as urban case B but with five times shorter branches ($L_1 = 0.5\,\text{km}$, $L_2 = 15.8\,\text{km}$, $L_3 = 13.1\,\text{km}$, $L_4 = 55.5\,\text{km}$, $L_5 = 15.1\,\text{km}$, $L_{b1} = 3.8\,\text{km}$, $L_{b2} = 4.5\,\text{km}$, $L_{b3} = 3.4\,\text{km}$, $L_{b4} = 3.6\,\text{km}$) —, and Topology 2 — same as urban case B but with five times longer branches ($L_1 = 0.5\,\text{km}$, $L_2 = 15.8\,\text{km}$, $L_3 = 13.1\,\text{km}$, $L_4 = 55.5\,\text{km}$, $L_5 = 15.1\,\text{km}$, $L_{b1} = 95\,\text{km}$, $L_{b2} = 113.5\,\text{km}$, $L_{b3} = 85.5\,\text{km}$, $L_{b4} = 90\,\text{km}$) —. In Figs. 7(b), 7(c), and 7(d), similar plots are given for the second, the third, and the fourth branch — points A_2, A_3, and A_4, respectively, see Fig. 3(a) —, respectively.

From Figs. 7(a), 7(b), 7(c), and 7(d), it should be mentioned that [29, 41, 74, 79, 85]:

- The attenuation discontinuity at each branch depends predominantly on its electrical length. It is verified that as the branches become longer, the spectral notches are reduced with regard both to their depth and to their spectral extent. Thus, the spectral behavior of the HV/BPL networks tends to converge to the spectral behavior of the N cascaded two-way power dividers.
- There may be amplification of the signal power (negative values of the attenuation discontinuity), depending on the HV network configuration. This has also been observed in MV/BPL transmission [41].

From the previous figures, several interesting conclusions concerning HV/BPL transmission characteristics may be deduced as follows.

1. As a broadband communications channel, the overhead HV power grid suffers primarily from "LOS" attenuation and secondarily from multipath which adversely affect the BPL system design and the oncoming SG application performance.
2. Though determined for 100 km long HV connections — compared to the shorter connections of LV and MV cases [2, 7, 21, 22, 28–32, 41–44, 86] —, BPL transmission via the overhead HV grid exhibits low loss characteristics favoring the exploitation of HV/BPL bandwidth.

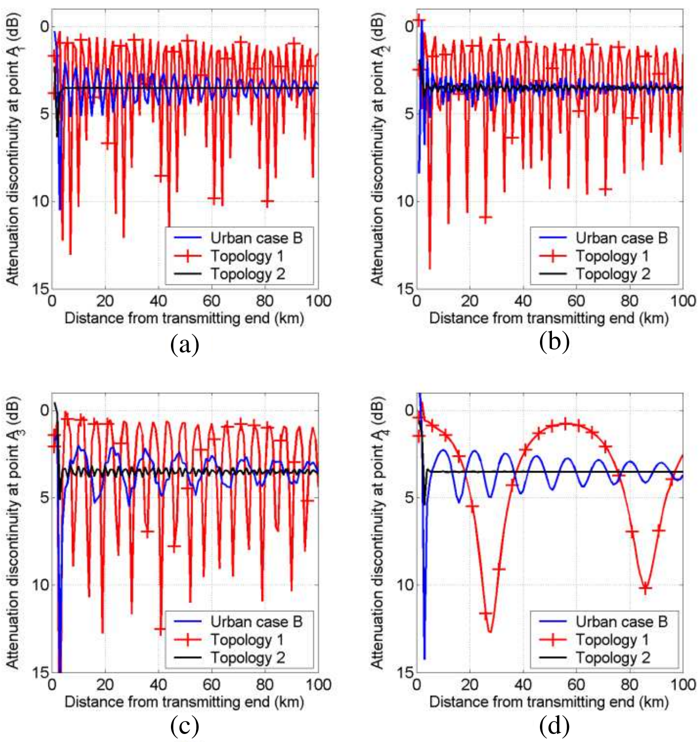

Figure 7. Attenuation discontinuity of DM_4 versus frequency for urban case B, Topology 1, and Topology 2. (The subchannel frequency spacing is equal to 1 MHz). (a) At the first branch — point A_1, see Fig. 3(a) —. (b) At the second branch — point A_2, see Fig. 3(a) —. (c) At the third branch — point A_3, see Fig. 3(a) —. (d) At the fourth branch — point A_4, see Fig. 3(a)—.

3. Besides the "LOS" attenuation, the overall end-to-end channel attenuation and the signal power discontinuities along the end-to-end transmission path of overhead HV/BPL systems depend on the frequency, the coupling scheme, and the number, the electrical length, and the termination of the various branches encountered along the end-to-end BPL signal propagation. Unlike channel attenuation, phase responses depend primarily on the frequency, the coupling scheme, and the "LOS" distance regardless of the overhead HV/BPL topology considered.
4. If the exact grid configuration is known, the overall spectral behavior may be accurately evaluated providing information about the necessity and the exact location where signal repeaters should

be installed and parameters of orthogonal frequency-division multiplexing (OFDM) systems used.

5. As usually done in BPL systems [28–30, 40, 84], overhead HV/BPL channels are classified into three classes depending on their spectral behavior: "LOS" channels; good channels; and bad channels. HV/BPL transmission in the majority of areas is classified into the good channels class.
6. In the SG landscape, overhead and underground LV/BPL, MV/BPL, and HV/BPL systems need to work in a compatible way (intraoperate) before BPL technology interoperates with other broadband technologies, such as wired (e.g., fiber and DSL) and wireless (e.g., WiFi and WiMax) [38, 88–90]. The comparable results concerning broadband signal transmission in LV/MV/HV BPL systems is the guarantee towards SG technology integration.

5. DISCUSSION AND CONCLUSIONS

The transmission characteristics of multiwire overhead HV/BPL networks have been studied applying the TM method. The broadband transmission capability of such networks depends on the frequency, the coupling scheme applied, the physical properties of the cables used, the MTL configuration, the end-to-end — "LOS" — distance, and the number and the electrical length of the branches encountered along the source-to-destination path. These factors determine the usable bandwidth, the position of repeaters, and the OFDM and various resource allocation schemes performance. The low loss nature of overhead HV/BPL systems permits the exploitation of HV/BPL bandwidth and provides with further LV/MV/HV BPL intraoperability options that may actually be of benefit towards a unified transmission/distribution SG power grid.

REFERENCES

1. Newbury, J., "Broadband power line communications for the electricity supply industry," *Proc. 2008 IEEE/PES Transmission and Distribution Conference and Exposition*, 1–8, T&D'08, Chicago, USA, Apr. 2008.
2. OPERA1, D44, Report Presenting the Architecture of PLC System, the Electricity Network Topologies, the Operating Modes and the Equipment over which PLC Access System Will be Installed, IST Integr. Project No 507667, Dec. 2005. Available: http://www.ist-opera.org/opera1/downloads/D44_Architecture_PLC.zip.

3. Pavlidou, N., A. H. Vinck, J. Yazdani, and B. Honary, "Power line communications: State of the art and future trends," *IEEE Commun. Mag.*, Vol. 41, No. 4, 3440, Apr. 2003.
4. Biglieri, E., S. Galli, Y. W. Lee, H. Poor, and H. Vinck, "Power line communications (Guest Editorial)," *IEEE J. Sel. Areas Commun.*, Vol. 24, No. 7, 1261–1266, Jul. 2006.
5. Galli, S., A. Scaglione, and Z. Wang, "For the grid and through the grid: The role of power line communications in the smart grid," *Proc. IEEE*, Vol. 99, No. 6, 998–1027, Jun. 2011.
6. Galli, S., A. Scaglione, and K. Dostert, "Broadband is power: Internet access through the power line network (Guest Editorial)," *IEEE Commun. Mag.*, Vol. 41, No. 5, 8283, May 2003.
7. Ferreira, H., L. Lampe, J. Newbury, and T. G. Swart, *Power Line Communications, Theory and Applications for Narrowband and Broadband Communications over Power Lines*, Wiley, New York, 2010.
8. Latchman, H. and L. Yonge, "Power line local area networking (Guest Editorial)," *IEEE Commun. Mag.*, Vol. 41, No. 4, 3233, Apr. 2003.
9. Prasanna, G. N. S., A. Lakshmi, S. Sumanth, V. Simha, J. Bapat, and G. Koomullil, "Data communication over the smart grid," *Proc. IEEE Int. Symp. Power Line Communications and Its Applications*, 273–279, Dresden, Germany, Mar./Apr. 2009.
10. NATO, "HF Interference, Procedures and tools (Interférences HF, procédures et outils) final report of NATO RTO information systems technology," RTO-TR-ISTR-050, Jun. 2007, Available: http://ftp.rta.nato.int/public/PubFullText/RTO/TR/RTO-TR-IST-050/TR-IST-050-ALL.pdf.
11. Anastasopoulos, M. P., A. C. Voulkidis, A. V. Vasilakos, and P. G. Cottis, "A secure network management protocol for Smart-Grid BPL networks: Design, implementation and experimental results," *Elsevier Computer Communications*, Vol. 31, No. 18, 4333–4342, Dec. 2008.
12. Aquilué, R., I. Gutierrez, J. L. Pijoan, and G. Sánchez, "High-voltage multicarrier spread-spectrum system field test," *IEEE Trans. Power Del.*, Vol. 24, No. 3, 1112–1121, Jul. 2009.
13. Aquilué, R., J. L. Pijoan, and G. Sánchez, "High voltage channel measurements and field test of a low power OFDM system," *Proc. IEEE Int. Symp. Power Line Communications and Its Applications*, 1–6, Jeju Island, South Korea, Apr. 2008.
14. Horowitz, S., A. Phadke, and B. Renz, "The future of power

transmission," *IEEE Power Energy Mag.*, Vol. 8, No. 2, 34–40, Mar. 2010.

15. US Department of Energy, "Broadband over power lines could accelerate the transmission smart grid," *Tech. Rep.*, DOE/NETL-2010/1418, 2010.
16. Moyo, N. M., N. B. Ijumba, and A. C. Britten, "Investigations on the noise generation phenomena in the PLC system of a long HVDC line," *Proc. Int. Conf. Power System Tech.*, 953–957, Kunming, China, Oct. 2002.
17. Suljanović, N., A. Mujčić, M. Zajc, and J. F. Tasič, "Corona noise characteristics in high voltage PLC channel," *Proc. Int. Conf. on Industrial Tech.*, Vol. 2, 1036–1039, Maribor, Slovenia, Dec. 2003.
18. Mujčić, A., N. Suljanović, M. Zajc, and J. F. Tasič, "Design of channel coding methods in HV PLC communications," *Proc. IEEE Int. Symp. Power Line Communications and Its Applications*, 379–384, Zaragoza, Spain, Mar./Apr. 2004.
19. Mujčić, A., N. Suljanović, M. Zajc, and J. F. Tasič, "High-voltage PLC roles in packet-switching networks of power utilities," *Proc. IEEE Int. Symp. Power Line Communications and Its Applications*, 204–209, Pisa, Italy, Mar. 2007.
20. Pighi, R. and R. Raheli, "On multicarrier signal transmission for high-voltage power lines," *Proc. IEEE Int. Symp. Power Line Commun. Appl.*, 32–36, Vancouver, BC, Canada, Apr. 2005.
21. DLC+VIT4IP, D1.2: Overall system architecture design DLC system architecture. FP7 Integrated Project No. 247750, Jun. 2010, Available: http://www.dlc-vit4ip.org/wb/media/Downloads/D1.2\%20system\%20architecture\%20design.pdf.
22. Dostert, K., *Powerline Communications*, Upper Saddle River, Prentice-Hall, NJ, 2001.
23. Suljanović, N., A. Mujčić, M. Zajc, and J. F. Tasič, "Computation of high-frequency and time characteristics of corona noise on HV power line," *IEEE Trans. Power Del.*, Vol. 20, No. 1, 71–79, Jan. 2005.
24. Suljanović, N., A. Mujčić, M. Zajc, and J. F. Tasič, "Integrated communication model of the HV power-line channel," *Proc. IEEE Int. Symp. Power Line Communications and Its Applications*, 79–84, Zaragoza, Spain, Mar./Apr. 2004.
25. Suljanović, N., A. Mujčić, M. Zajc, and J. F. Tasič, "Approximate computation of high-frequency characteristics for power line with horizontal disposition and middle-phase to ground coupling,"

Elsevier Electr. Power Syst. Res., Vol. 69, 17–24, Jan. 2004.

26. Bakshi, U. A. and M. V. Bakshi, *Generation, Transmission and Distribution*, Technical Publications Pune, Pune, India, 2001.
27. De Sosa, J. C., *Analysis and Design of High-voltage Transmission Lines*, iUniverse Incorporated, Bloomington, IN, USA, 2010.
28. Lazaropoulos, A. G. and P. G. Cottis, "Capacity of overhead medium voltage power line communication channels," *IEEE Trans. Power Del.*, Vol. 25, No. 2, 723–733, Apr. 2010.
29. Lazaropoulos, A. G. and P. G. Cottis, "Broadband transmission via underground medium-voltage power lines — Part I: Transmission characteristics," *IEEE Trans. Power Del.*, Vol. 25, No. 4, 2414–2424, Oct. 2010.
30. Lazaropoulos, A. G. and P. G. Cottis, "Broadband transmission via underground medium-voltage power lines — Part II: Capacity," *IEEE Trans. Power Del.*, Vol. 25, No. 4, 2425–2434, Oct. 2010.
31. Gebhardt, M., F. Weinmann, and K. Dostert, "Physical and regulatory constraints for communication over the power supply grid," *IEEE Commun. Mag.*, Vol. 41, No. 5, 84–90, May 2003.
32. Henry, P. S., "Interference characteristics of broadband power line communication systems using aerial medium voltage wires," *IEEE Commun. Mag.*, Vol. 43, No. 4, 92–98, Apr. 2005.
33. Liu, S. and L. J. Greenstein, "Emission characteristics and interference constraint of overhead medium-voltage broadband power line (BPL) systems," *Proc. IEEE Global Telecommunications Conf.*, 1–5, New Orleans, LA, USA, Nov./Dec. 2008.
34. Götz, M., M. Rapp, and K. Dostert, "Power line channel characteristics and their effect on communication system design," *IEEE Commun. Mag.*, Vol. 42, No. 4, 78–86, Apr. 2004.
35. Fenton, D. and P. Brown, "Some aspects of benchmarking high frequency radiated emissions from wireline communications systems in the near and far fields," *Proc. IEEE Int. Symp. on Power Line Communications and Its Applications*, 161–167, Malmö, Sweden, Apr. 2001.
36. Fenton, D. and P. Brown, "Modelling cumulative high frequency radiated interference from power line communication systems," *Proc. IEEE Int. Conf. on Power Line Communications and Its Applications*, Athens, Greece, Mar. 2002.
37. Zimmermann, M. and K. Dostert, "A multipath model for the powerline channel," *IEEE Trans. Commun.*, Vol. 50, No. 4, 553–559, Apr. 2002.

38. Galli, S. and O. Logvinov, "Recent developments in the standardization of power line communications within the IEEE," *IEEE Commun. Mag.*, Vol. 46, No. 7, 64–71, Jul. 2008.
39. Tonello, A. M. and F. Pecile, "Efficient architectures for multiuser FMT systems and application to power line communications," *IEEE Trans. Commun.*, Vol. 57, No. 5, 1275–1279, May 2009.
40. Versolatto, F. and A. M. Tonello, "An MTL theory approach for the simulation of MIMO power-line communication channels," *IEEE Trans. Power Del.*, Vol. 26, No. 3, 1710–1717, Jul. 2011.
41. Lazaropoulos, A. G. and P. G. Cottis, "Transmission characteristics of overhead medium voltage power line communication channels," *IEEE Trans. Power Del.*, Vol. 24, No. 3, 1164–1173, Jul. 2009.
42. Amirshahi, P. and M. Kavehrad, "High-frequency characteristics of overhead multiconductor power lines for broadband communications," *IEEE J. Sel. Areas Commun.*, Vol. 24, No. 7, 1292–1303, Jul. 2006.
43. Sartenaer, T., "Multiuser communications over frequency selective wired channels and applications to the power-line access network," Ph.D. Dissertation, Univ. Catholique Louvain, Louvain-la-Neuve, Belgium, Sep. 2004, Available: http://www.tele.ucl.ac.be/ts/PhD.php.
44. Calliacoudas, T. and F. Issa, "'Multiconductor transmission lines and cables solver,' An efficient simulation tool for plc channel networks development," *IEEE Int. Conf. Power Line Communications and Its Applications*, Athens, Greece, Mar. 2002.
45. Galli, S. and T. Banwell, "A deterministic frequency-domain model for the indoor power line transfer function," *IEEE J. Sel. Areas Commun.*, Vol. 24, No. 7, 1304–1316, Jul. 2006.
46. Galli, S. and T. Banwell, "A novel approach to accurate modeling of the indoor power line channel — Part II: Transfer function and channel properties," *IEEE Trans. Power Del.*, Vol. 20, No. 3, 1869–1878, Jul. 2005.
47. Paul, C. R., *Analysis of Multiconductor Transmission Lines*, Wiley, New York, 1994.
48. Faria, J. A. B., *Multiconductor Transmission-line Structures: Modal Analysis Techniques*, Wiley, New York, 1994.
49. Sartenaer, T. and P. Delogne, "Deterministic modelling of the (Shielded) outdoor powerline channel based on the multiconductor transmission line equations," *IEEE J. Sel. Areas Commun.*, Vol. 24, No. 7, 1277–1291, Jul. 2006.

50. Sartenaer, T. and P. Delogne, "Powerline cables modelling for broadband communications," *Proc. IEEE Int. Conf. Power Line Communications and Its Applications*, 331–337, Malmö, Sweden, Apr. 2001.
51. Pérez, A., A. M. Sánchez, J. R. Regué, M. Ribó, R. Aquilué, P. Rodréguez-Cepeda, and F. J. Pajares, "Circuital and modal characterization of the power-line network in the PLC band," *IEEE Trans. Power Del.*, Vol. 24, No. 3, 1182–1189, Jul. 2009.
52. Meng, H., S. Chen, Y. L. Guan, C. L. Law, P. L. So, E. Gunawan, and T. T. Lie, "Modeling of transfer characteristics for the broadband power line communication channel," *IEEE Trans. Power Del.*, Vol. 19, No. 3, 1057–1064, Jul. 2004.
53. Philipps, H., "Modelling of powerline communications channels," *Proc. IEEE Int. Symp. Power Line Communications and Its Applications*, 14–21, Lancaster, UK, Mar./Apr. 1999.
54. Anastasiadou, D. and T. Antonakopoulos, "Multipath characterization of indoor power-line networks," *IEEE Trans. Power Del.*, Vol. 20, No. 1, 90–99, Jan. 2005.
55. Amirshahi, P., "Broadband access and home networking through powerline networks," Ph.D. Dissertation, Pennsylvania State Univ., University Park, PA, May 2006, Available: http://etda.libraries.psu.edu/theses/approved/WorldWideIndex/ETD-1205/index.html.
56. Barmada, S., A. Musolino, and M. Raugi, "Innovative model for time-varying power line communication channel response evaluation," *IEEE J. Sel. Areas Commun.*, Vol. 24, No. 7, 1317–1326, Jul. 2006.
57. D'Amore, M. and M. S. Sarto, "A new formulation of lossy ground return parameters for transient analysis of multiconductor dissipative lines," *IEEE Trans. Power Del.*, Vol. 12, No. 1, 303–314, Jan. 1997.
58. Suljanović, N., A. Mujčić, M. Zajc, and J. F. Tasič, "High-frequency characteristics of high-voltage power line," *Proc. IEEE Int. Conf. on Computer as a Tool*, 310–314, Ljubljana, Slovenia, Sep. 2003.
59. Suljanović, N., A. Mujčić, M. Zajc, and J. F. Tasič, "Power-line high-frequency characteristics: analytical formulation," *Proc. Joint 1st Workshop on Mobile Future & Symposium on Trends in Communications*, 106–109, Bratislava, Slovakia, Oct. 2003.
60. Villiers, W., J. H. Cloete, and R. Herman, "The feasibility of ampacity control on HV transmission lines using the PLC system," *Proc. IEEE Conf. Africon*, Vol. 2, 865–870, George, South Africa,

Oct. 2002.

61. Zajc, M., N. Suljanović, A. Mujčić, and J. F. Tasič, "Frequency characteristics measurement of overhead high-voltage power-line in low radio-frequency range," *IEEE Trans. Power Del.*, Vol. 22, No. 4, 2142–2149, Oct. 2007.
62. Amirshahi, P. and M. Kavehrad, "Medium voltage overhead powerline broadband communications; Transmission capacity and electromagnetic interference," *Proc. IEEE Int. Symp. Power Line Commun. Appl.*, 2–6, Vancouver, BC, Canada, Apr. 2005.
63. D'Amore, M. and M. S. Sarto, "Simulation models of a dissipative transmission line above a lossy ground for a wide-frequency range — Part I: Single conductor configuration," *IEEE Trans. Electromagn. Compat.*, Vol. 38, No. 2, 127–138, May 1996.
64. D'Amore, M. and M. S. Sarto, "Simulation models of a dissipative transmission line above a lossy ground for a wide-frequency range — Part II: Multi-conductor configuration," *IEEE Trans. Electromagn. Compat.*, Vol. 38, No. 2, 139–149, May 1996.
65. Anatory, J. and N. Theethayi, "On the efficacy of using ground return in the broadband power-line communications-A transmission-line analysis," *IEEE Trans. Power Del.*, Vol. 23, No. 1, 132–139, Jan. 2008.
66. Carson, J. R., "Wave propagation in overhead wires with ground return," *Bell Syst. Tech. J.*, Vol. 5, 539–554, 1926.
67. Kikuchi, H., "Wave propagation along an infinite wire above ground at high frequencies," *Proc. Electrotech. J.*, Vol. 2, 73–78, Dec. 1956.
68. Kikuchi, H., "On the transition form a ground return circuit to a surface waveguide," *Proc. Int. Congr. Ultrahigh Frequency Circuits Antennas*, 39–45, Paris, France, Oct. 1957.
69. Issa, F., D. Chaffanjon, E. P. de la Bâthie, and A. Pacaud, "An efficient tool for modal analysis transmission lines for PLC networks development," *IEEE Int. Conf. Power Line Communications and Its Applications*, Athens, Greece, Mar. 2002.
70. Villiers, W., J. H. Cloete, L. M. Wedepohl, and A. Burger, "Real-time sag monitoring system for high-voltage overhead transmission lines based on power-line carrier signal behavior," *IEEE Trans. Power Del.*, Vol. 23, No. 1, 389–395, Jan. 2008.
71. Lodwig, S. G. and C. C. Schuetz, "Coupling to control cables in HV substations," *Proc. IEEE Int. Symp. ElectroMagentic Compatibility*, 249–253, Montreal, Canada, Mar. 2001.
72. Van der Wielen, P. C. J. M., "On-line detection and lo-

cation of partial discharges in medium-voltage power cables" Ph.D. Dissertation, Eindhoven University of Technology, Eindhoven, the Netherlands, Apr. 2005, Available: http://alexandria.tue.nl/extra2/200511097.pdf.

73. Wouters, P. A. A. F., P. C. J. M. van der Wielen, J. Veen, P. Wagenaars, and E. F. Steennis, "Effect of cable load impedance on coupling schemes for MV power line communication," *IEEE Trans. Power Del.*, Vol. 20, No. 2, Part 1, 638–645, Apr. 2005.
74. Anatory, J., N. Theethayi, R. Thottappillil, M. M. Kissaka, and N. H. Mvungi, "The influence of load impedance, line length, and branches on underground cable Power-Line Communications (PLC) systems," *IEEE Trans. Power Del.*, Vol. 23, No. 1, 180–187, Jan. 2008.
75. Yarman, B. S. and A. Fettweiss, "Computer aided double matching via parametric representation of Brune functions," *IEEE Trans. Circuits Syst.*, Vol. 37, No. 2, 212–222, Feb. 1990.
76. Araneo, R., S. Celozzi, G. Lovat, and F. Maradei, "Multi-port impedance matching technique for power line communications," *Proc. IEEE Int. Symp. Power Line Communications and Its Applications*, 96–101, Udine, Italy, Apr. 2011.
77. Papadopoulos, T. A., B. D. Batalas, A. Radis, and G. K. Papagiannis, "Medium voltage network PLC modeling and signal propagation analysis," *Proc. IEEE Int. Symp. Power Line Communications and Its Applications*, 284–289, Pisa, Italy, Mar. 2007.
78. Fortunato, E., A. Garibbo, and L. Petrolino, "An experimental system for digital power line communications over high voltage electric power lines — Field trials and obtained results," *Proc. IEEE Int. Symp. Power Line Communications and Its Applications*, 26–31, Kyoto, Japan, Mar. 2003.
79. Anatory, J., N. Theethayi, and R. Thottappillil, "Power-line communication channel model for interconnected networks — Part II: Multiconductor system," *IEEE Trans. Power Del.*, Vol. 24, No. 1, 124–128, Jan. 2009.
80. Pang, T. S., P. L. So, K. Y. See, and A. Kamarul, "Modeling and analysis of common-mode current propagation in broadband power-line communication networks," *IEEE Trans. Power Delivery*, Vol. 23, No. 1, 171–179, Jan. 2008.
81. Vukicevic, A., M. Rubinstein, F. Rachidi, and J. L. Bermudez, "On the mechanisms of differential-mode to common-mode conversion in the broadband over power line (BPL) frequency band," *Proc. 2006 International Zurich Symposium on Electromagnetic Compatibility*, 658–661, Zurich, Switzerland, Feb. 2006.

82. FCC, "In the Matter of Amendment of Part 15 Regarding New Requirements and Measurement Guidelines for Access Broadband over Power Line Systems," FCC 04-245 Report and Order, Jul. 2008, Available: http://www.fcc.gov/oet/info/rules/part15/PART15_07-10-08.pdf.
83. NTIA, "Potential interference from broadband over power line (BPL) systems to federal government radio communications at 1.7–80 MHz Phase 1 Study Vol. 1," NTIA Rep. 04-413, Apr. 2004, Available: http://www.ntia.doc.gov/ntiahome/fccfilings/2004/bpl/.
84. Kuhn, L. M., S. Berger, I. Hammerström, and A. Wittneben, "Power line enhanced cooperative wireless communications," *IEEE J. Sel. Areas Commun.*, Vol. 24, No. 7, 1401–1410, Jul. 2006.
85. Anatory, J., N. Theethayi, R. Thottappillil, M. M. Kissaka, and N. H. Mvungi, "The effects of load impedance, line length, and branches in typical low-voltage channels of the BPLC systems of developing countries: Transmission-line analyses," *IEEE Trans. Power Del.*, Vol. 24, No. 2, 621–629, Apr. 2009.
86. OPERA1, D5: Pathloss as a Function of Frequency, Distance and Network Topology for Various LV and MV European Powerline Networks. IST Integrated Project No 507667, Apr. 2005, Available: http://www.ist-opera.org/opera1/downloads/D5/D5_Pathloss.pdf.
87. Galli, S., Y. Masuda, and Y. Urabe, "Time reuse algorithms: A novel approach to solving the issue of scalability in dense power line networks," *Proc. IEEE Int. Symp. Power Line Communications and Its Applications*, 101–106, Dresden, Germany, Mar./Apr. 2009.
88. Gellings, C. W., M. Samotyj, and B. Howe, "The futures power delivery system," *IEEE Power Energy Mag.*, Vol. 2, No. 5, 4048, Sep./Oct. 2004.
89. Galli, S., A. Kurobe, and M. Ohura, "The inter-PHY protocol (IPP): A simple coexistence protocol for shared media," *Proc. IEEE Int. Symp. Power Line Communications and Its Applications*, 194–200, Dresden, Germany, Mar./Apr. 2009.
90. Arlandis, D., J. Barbero, A. Matas, S. Iranzo, J. C. Riveiro, and D. Ruiz, "Coexistence in PLC networks," *IEEE Int. Symp. on Power Line Communications and Its Applications*, 260–264, Vancouver, Canada, Apr. 2005.